The novel oncolytic adenoviral mutant Ad5-3Δ-A20T retargeted to $\alpha_v\beta_6$-integrins efficiently eliminates pancreatic cancer cells

Y. K. Stella Man[1], James A. Davies[3], Lynda Coughlan[4], Constantia Pantelidou[5], Alfonso Blázquez-Moreno[6], John F. Marshall[2], Alan L. Parker[3], Gunnel Halldén[1]*

Affiliations: [1]Centre for Molecular Oncology and [2]Centre for Tumour Biology, Barts Cancer Institute, Queen Mary University of London, UK. [3]Division of Cancer and Genetics, School of Medicine, Cardiff University, Cardiff, UK. [4]Department of Microbiology, Icahn School of Medicine at Mount Sinai, New York, NY, USA. [5]Medical Oncology, Dana Farber Cancer Institute, Boston, MA, USA. [6]Department of Immunology and Oncology, Centro Nacional de Biotecnología-Consejo Superior de Investigaciones Científicas, Madrid, Spain.

Running Title: Novel oncolytic adenovirus retargeted to αvβ6-integrins

Key words: PDAC; 3-dimensional culture; organotypic; *in vivo* model; oncolytic adenovirus

[*]Contact information for corresponding author:

Dr Gunnel Halldén

Reader Cancer Gene Therapy, Centre for Molecular Oncology
Barts Cancer Institute - a Cancer Research UK Centre of Excellence
Queen Mary, University of London
John Vane Science Centre, Charterhouse Square, London EC1M 6BQ
Tel: +44 (0)20 7882 3593
Email: g.hallden@qmul.ac.uk

Conflict of interest:

The authors declare that they have no conflict of interest.

Grant support

This study was supported by generous grants from the UK Charity Pancreatic Cancer Research Fund (PCRF) and the BCI CRUK Centre Grant [grant number C16420/A18066] (G. Halldén, S. Man, C. Pantelidou), and the CRUK Biotherapeutics Drug Discovery Project Award [grant number 23946] (A.Parker, J. Davies).

Abstract

Metastatic pancreatic ductal adenocarcinomas (PDAC) are incurable due to the rapid development of resistance to all current therapeutics. Oncolytic adenoviral mutants have emerged as a promising new strategy that negates such resistance. In contrast to normal tissue, the majority of PDAC express the αvβ6-integrin receptor. To exploit this feature, we modified our previously reported oncolytic adenovirus, AdΔΔ to selectively target αvβ6-integrins to facilitate systemic delivery. Structural modifications to AdΔΔ include the expression of the small but potent αvβ6-binding peptide, A20FMDV2 and ablation of binding to the native Coxsackie and Adenovirus Receptor (CAR) within the fibre knob region. The resultant mutant, Ad-3Δ-A20T infected and killed αvβ6-integrin expressing cells more effectively than the parental wild type (Ad5wt) virus and AdΔΔ. Viral uptake through αvβ6-integrins rather than native viral receptors (CAR, αvβ3- and αvβ5-integrins) promoted viral propagation and spread. Superior efficacy of Ad-3Δ-A20T compared to Ad5wt was demonstrated in 3D organotypic co-cultures, and similar potency between the two viruses was observed in Suit-2 *in vivo* models. Importantly, Ad-3Δ-A20T infected pancreatic stellate cells at low levels, which may further facilitate viral spread and cancer cell elimination either as a single agent or in combination with the chemotherapy drug, gemcitabine. We demonstrate that Ad-3Δ-A20T is highly selective for αvβ6-integrin expressing pancreatic cancer cells and with further development, this new and exciting strategy can potentially be extended to improve the systemic delivery of adenoviruses to pancreatic cancer patients.

Introduction

Pancreatic ductal adenocarcinomas (PDAC) are aggressive cancers with high mortality and low 5-year survival rates globally (1). Major reasons for the dismal prognosis are the late presentation of symptoms and the rapid development of resistance to all current therapeutics that do not significantly prolong survival (1, 2). Replication-selective oncolytic adenoviruses efficiently target all epithelial cancers including treatment-resistant pancreatic cancer cells and have excellent safety records in early phase clinical trials. The first oncolytic adenoviral mutant to be evaluated in pancreatic cancer patients was Onyx-015 (*dl*1520) with deletion of the E1B55K gene enabling virus-propagation in cancer cells with aberrant nuclear mRNA export and non-functional p53 (3-5). Despite proven safety in two Phase I trials in conjunction with gemcitabine, efficacy was limited because essential viral functions were compromised by the deletion. More recently, mutants with higher efficacy have been developed by deleting the small pRb-binding E1ACR2-region (ΔCR2) that prevent replication in normal tissue while viral propagation and spread in tumour cells is complemented by deregulated cell cycle control (pRb-p16 regulation) (6-8). The most common genetic alterations in pancreatic cancer are activating *KRAS* mutations, *CDKN2A/p16* deletion, and inactivating *TP53* mutations (9) and consequently, replication of E1AΔCR2 mutants readily proceeds. E1AΔCR2 mutants have not yet been evaluated in PDAC patients while promising outcomes were reported in gliomas and osteosarcomas with Ad5ΔCR2-variants (8, 10).

We recently developed the novel mutant AdΔΔ with the anti-apoptotic E1B19K gene deleted in addition to the E1ACR2-deletion (6, 11, 12). E1B19K is a functional Bcl-2 homologue that binds Bax and Bak, and inhibits mitochondrial pore formation and apoptosis in response to death receptor-activation and intrinsically induced apoptosis (13). AdΔΔ synergized with the current clinical standard of care for pancreatic cancer, gemcitabine and irinotecan, without toxicity to normal cells (6, 11, 14). However, to efficiently target pancreatic cancer lesions in patients by systemic administration required further modifications. Human erythrocytes express high levels of the native viral receptor, Coxsackie and Adenovirus Receptor (CAR) and Complement Receptor 1 (CR-1) that bind the viral fibre knob in the presence of neutralizing antibodies and complement, resulting in lower doses of virus reaching the tumour (15). Other barriers to systemic delivery are the rapid elimination of virus by hepatic Kupffer

cells and hepatocyte uptake, and the high affinity binding to numerous blood factors (16-18). For example, Factor X (FX) binds to the viral hexon protein and bridges the virus to heparan sulfate proteoglycans (HSPGs) mainly on the hepatocyte surface and promotes liver transduction (17). Factor IX (FIX) has also been reported to aid the transduction of hepatocytes although, it remains unclear which viral protein is responsible, and complement-4 binding protein (C4BP) binds to the fibre knob (16, 18). Importantly, viral binding to blood factors rapidly induces innate immune activation to the vector resulting in systemic inflammatory responses in patients (18, 19). We hypothesised that the local viral concentration at tumour sites could be increased by, i) targeting of mutants to pancreatic tumours and, ii) decreasing binding to erythrocytes and blood factors. Ultimately, we generated a novel oncolytic adenovirus modified to improve tumour targeting.

The αvß6-integrin is highly expressed in many solid tumours but not in normal cells (20-22). To take advantage of the selective expression of αvß6-integrin in PDAC cells, we previously generated the retargeted wild type mutants Ad5A20 and Ad5A20-477*dl*TAYT (23, 24). The mutants were engineered to express a 20 amino acid peptide A20FMDV2 derived from the foot-and-mouth disease virus (FMDV) that selectively binds through an Arg-Gly-Asp (RGD)-domain to αvß6 (25, 26). Ad5-A20477*dl*TAYT was also modified to reduce CAR and complement binding and partially relieved some of the obstacles with systemic delivery by reducing erythrocyte binding (23, 24).

In this study we report on the generation of a novel mutant, Ad5-3Δ-A20T based on the oncolytic mutant AdΔΔ, with incorporation of the A20FMDV2 peptide, ablation of CAR binding and deletion of E3gp19K, for optimal replication-selectivity, cancer targeting and immune stimulation. Ad5-3Δ-A20T potently replicated in and killed cultured PDAC cells, in xenografts *in vivo* and in 3-dimensional co-culture models with pancreatic stellate cells. Ad5-3Δ-A20T was highly efficacious and retained all viral functions necessary for propagation in pancreatic cancer cells also in the presence of gemcitabine. We expect these findings to guide further optimisation of oncolytic adenoviruses for systemic delivery to improve on therapeutic efficacy in patients with pancreatic cancer in conjunction with current treatments.

Materials and Methods

Cell lines and culture conditions

Human pancreatic ductal adenocarcinoma (PDAC) cell lines were used in the study: BxPC-3, Panc04.03, Capan-2, PANC-1, and MiaPaCa-2 (primary tumours); CFPAC-1 and Capan-1 (liver metastasis), Hs766t (lymph node metastasis) (ATCC, LGC Standards, UK), and Suit-2, PaTu8902 and PaTu8988t (liver metastasis) and PaTu8988s (primary tumour) (Cell Services, Cancer Research UK). The PT45 cells (primary tumour) were a kind gift from Prof H. Kalthoff (Comprehensive Cancer, Campus Kiel, Germany). The hTERT-immortalised human pancreatic stellate cells (PS1) were a kind gift from Prof. H. Kocher (BCI, QMUL, London) (27). The human embryonic kidney cells HEK293 and JH293 (Cell Services, Cancer Research UK) and the human lung carcinoma cells A549 (LGC Standards, UK) were used for viral production. Cells were grown at 37°C and 5% CO_2 in Dulbecco Modified Eagle's medium (DMEM) supplemented with 10% Fetal Bovine Serum (FBS) and 1% penicillin and streptomycin (Penicillin 10000 units/ml, Streptomycin 10mg/ml; P/S) (Sigma-Aldrich, MO). All cell lines were STR-profiled (LGC Standards, UK and Cancer Research UK) and verified to be identical to the profiles reported by the suppliers and to the original vial.

Organotypic 3-dimensional (3D) co-culture models

The development of the 3-dimensional co-culture models (organotypic cultures) for pancreatic adenocarcinoma cells and stromal cells has been previously described in detail elsewhere (27-29). Briefly, collagen type I was mixed with Matrigel at different ratios, typically 3:1, in Transwells® (Corning; Sigma-Aldrich) and placed in 24-well plates. Panc0403 or Suit-2 cells were seeded together with PS1 cells (typical ratio 1:2; total $1x10^5$cells/well) on top of gels in 10% FBS Ham's F12/DMEM (GIBCO). After 24h the media in the top-chamber was replaced with serum-free DMEM, 3-4 days later viruses were added at 2-5-fold higher doses than in regular 2D-cultures and fixed in formalin 4-7days later. In some studies cells were embedded within the gels and virus added either in the top or bottom compartment. In combination studies gemcitabine (Gemzar; Eli Lilly, IN) was added at 5-10nM in serum-free DMEM on top of gel and/or in 10% FBS Ham's F12/DMEM underneath the transwell.

Viruses and infections

Wild-type virus Ad5 and the modified EGFP-expressing mutants, Ad5, Ad5A20 and Ad5A20-477*dl*TAYT were previously generated from species C wild-type adenovirus type 5 (23, 24). Briefly a 20-amino acid RGD-binding peptide (A20FMDV2; NAVPNLRGD*LQVLAQKVART* (26)) from VP1 of the foot-and-mouth disease virus (FMDV) (30) was incorporated in the HI-loop of the Ad5 fibre knob in Ad5A20 (23). Ad5A20 was further modified to generate Ad5A20-477*dl*TAYT through a base substitution Y477A and a deletion of amino acids 489-492 (TAYT) in the fibre knob and the E3gp19K gene was replaced by EGFP (18, 24, 31). Generation of AdΔΔ (deleted in E1ACR2 and E1B19K) has previously been described (6, 12). Ad5-3Δ-A20477*dl*TAYT (Ad5-3Δ-A20T) was generated by two-step homologous recombination in SW102 bacteria (32, 33). The wild-type Ad5 genome previously captured within a bacterial artificial chromosome (BAC) was modified in a series of stages (primer sequences; Supplementary Table 1). First, the wild type E1 genes were replaced with the PCR amplified modified E1-region from AdΔΔ. Next, the fibre knob domain of Ad5A20-477*dl*TAYT was PCR amplified and inserted to replace the wild-type knob. Finally, the E3gp19K domain was deleted generating Ad5-3Δ-A20T. The viruses were produced, purified and characterised according to standard protocols (6, 12). The viral particle (vp) to infectious unit (plaque-forming units; pfu) was 9-45vp/pfu for all viruses with the highest ratios for the FMDV expressing mutants. All infections were performed in serum-free DMEM and 2h later the media was replaced with 10% FBS/1% P/S DMEM ± the indicated doses of drugs.

Cell viability assay

Cells were infected with viral mutants in 2% FBS/1% P/S DMEM and were assayed 72h or 96h later using the 3-(4,5-dimethylthiazol-2-yl)-5-(3-carboxymethoxyphenyl)-2-(4-sulfophenyl)-2H-tetrazolium assay (MTS; Promega, Southampton, UK) to quantify live cells as an indirect measurement of cell death. Dose–response curves were generated to determine the concentration of each virus killing 50% of cells (EC_{50}) using untreated cells as controls. Each data point was generated from triplicate samples and experiments repeated at least three times as described previously (12).

Viral genome amplification by qPCR

Cells were infected with 100 particles per cell (ppc) of the respective virus and were harvested 4, 24, 48 and 72h later. The cell suspensions were pelleted, snap-frozen and stored at -80ºC. DNA was extracted using the QIAamp DNA Blood Mini Kit, according to the manufacturer's instructions (Qiagen, Netherlands) and used for quantitative PCR (qPCR) analysis as previously described (11, 14).

Viral replication assay by tissue culture infectious dose ($TCID_{50}$)

Cells were infected as described for qPCR and cells and media were collected at the indicated time points, freeze-thawed, and analyzed by the $TCID_{50}$ limiting dilution method on JH293 or A549 cells. Ad5 wild type virus of known activity was included in every assay as internal control as previously described (14).

Quantification of infectivity and cell surface receptor levels

Cells were seeded ($1x10^5$cells/well) in 6-well plates 24h prior to infection with the EGFP-expressing mutants at 100 or 500ppc in serum free DMEM, 2h later media was replaced with 10% FBS/DMEM. Viral infectivity was quantified by flow cytometry analysis (FACs) using EGFP expression as a marker, 48h and 72h post-infection. Cells were detached with trypsin/EDTA and combined with non-attached cells in the media and re-suspended in cold FACS buffer (0.1% BSA/DMEM).

To quantify cell-surface receptors cells were grown and treated as described above, re-suspended and incubated on ice for 1h with the respective primary mouse monoclonal antibody; anti-Coxsackie and Adenovirus Receptor (anti-CAR at 1:1000; ATCC), anti-αvβ3-integrin (1:100; Chemicon), anti-αvβ5 (1:100; Cancer Research UK) and anti-αvβ6 (1:100; Clone 10D5, Millipore). Bound antibodies were detected with secondary goat anti-mouse IgG conjugated to fluorescein isothiocyanate (FITC; Alexaflour 488 at 1:250; Molecular Probes) for 1h. To determine the role of each receptor, antibodies targeting αvβ5 or αvβ6 (at 1:100) or the A20FMDV2 peptide (10nM) were incubated with the cells for 10min on ice prior to the addition of virus.

EGFP expression and cell surface protein levels were determined by detection of fluorescence on the FACSCalibur instrument acquiring 10,000 events per sample and analyzed using the FlowJo software 8.8.6 (Tree Star Inc.).

Immunohistochemistry (IHC)

Formalin fixed paraffin embedded cells, organotypic cultures or tissue sections (10µm) were dewaxed, rehydrated in decreasing ethanol concentrations, water and PBS. Antigen retrieval was performed by boiling in 10mM Sodium Citrate Buffer pH6 for 8min, followed by water and PBS at 24°C. Cell permeabilisation was for 5 min in 0.2% Triton-X/PBS in blocking buffer (2% BSA/10% FBS/PBS). Primary antibodies, αSMA (1:300; M0851, Dako) and E1A (1:500; M58, GeneTex) were incubated overnight at 4°C, followed by fluorescent-labeled secondary anti-mouse antibodies for 1h (1:500; Alexa Fluor 488, ThermoFisher). Sections were stained with 4',6'-diamidino-2-phenylindole (DAPI, 1mg/ml; ThermoFisher), mounted with FluorSave Reagent (Calbiochem), stored at -20°C and analysed by confocal microscopy (Zeiss 710).

Tumours were harvested at the end of the study and fixed in 4% formaldehyde. The fixed tissues were sectioned and processed for histopathology with hematoxylin and eosin (H/E) and for IHC by staining for E1A and hexon (1:2000; AutogenBioclear) followed by detection using HRP-conjugated secondary antibodies (Dako).

In vivo tumor growth

Tumor cells were inoculated subcutaneously in one flank of CD*nu/nu* athymic mice (Charles River, UK) with Suit-2 cells in sterile PBS ($1x10^6$cells/200µl). Treatments were initiated when tumor volumes reached 100±20µl (14 days after inoculation) by intratumoural administration of adenoviral mutants at doses ranging from $1x10^8$ - $3x10^9$vp/injection, on day 1, 3 and 6 or day 1, 3, 5, 7 and 9. Tumor growth, progression and animal weight were followed until tumors reached 1.44cm^2 or until symptomatic tumor ulceration occurred (according to UK Home Office Regulations). Tumor volumes were estimated twice weekly: volume = (length x width^2 x π)/6 and growth curves were compared using one-way Anova. Survival analysis was performed according to the method of Kaplan-Meier (log rank test for statistical significance). Each treatment group included 8 animals and studies were performed twice according to two protocols as described above. For viral distribution studies, virus was administered via the tail vein with a single injection of $3x10^9$vp in 100µl. Tumours were harvested 24, 48 and 72h later, sonicated, and protein expression determined by Western blotting (Supplementary Materials and Methods). E1A was

detected by mouse anti-E1A (1:500; M58, GeneTex) and PCNA by mouse anti-PCNA (1:1000; Santa Cruz Biotech).

Results

Pancreatic cancer cells express higher levels of αvß6-integrin than Coxsackie Adenovirus Receptor (CAR) and are more susceptible to infection with A20FMDV2-retargeted mutants than with Adwt.

Pancreatic tumours frequently express the αvß6-integrin, reported to play a role in the progression of pancreatic cancer (21, 34). A panel of 15 human pancreatic cancer cell lines was screened for αvß6-integrin expression to determine the feasibility of retargeting the replication-selective AdΔΔ to this integrin. Expression levels were high in the majority of cell lines while levels of the native adenovirus receptor CAR, were consistently low compared to the JH293 cells (Fig. 1A and Supplementary Fig. 1A). The degree of infectivity with the FMDV2-expressing Ad5A20 (targeting αvß6 and CAR) and Ad5A20-477*dl*TAYT (targeting αvß6 only) was markedly higher than with wild type Ad5 (Ad5wt; targeting CAR only) across all cell lines that expressed the αvß6-integrin (Fig. 1A-B and Supplementary Fig. 1B). Infection levels strongly correlated with αvß6-integrin expression (R^2=0.7; Fig. 1C). In contrast, no correlation was obtained between Ad5A20- or Ad5A20-477*dl*TAYT-infection and CAR-levels or between Ad5wt-infection and αvß6-integrin expression levels ($R^2 \leq 0.2$; Supplementary Fig. 1C-D).

After the initial screening of 15 cell lines, we selected 5 of these for further in depth studies that represented a range of αvß6-integrin expression levels; PT45 low, Panc04.03 high, and MiaPaca-2, Suit-2, and BxPC-3 intermediate (Fig. 1A). Infection in Suit-2 and Panc04.03 cells were significantly higher with Ad5A20 and Ad5A20-477*dl*TAYT compared to infection with Ad5wt ($p<0.05$; Suit-2 and $p<0.01$; Panc04.03) (Fig. 2A). A similar trend was observed in BxPC-3 cells while in MiaPaCa-2 or PT45 cells all viruses infected to a similar degree. Infection levels in all five cell lines strongly correlated with the expression levels of αvß6-integrin (Ad5A20, R^2=0.99; Fig. 2B). The A20FMDV2-expressing mutants caused significantly higher levels of cell killing in Suit-2 and Panc04.03 cells compared to Ad5wt ($p \leq 0.05$) but not in PT45, MIA PaCa-2a or BxPC-3 (Fig. 2C). The BxPC-3

cells were the most sensitive to Adwt infection with the lowest EC_{50}-values of all tested cell lines (Supplementary Table 2). Despite higher levels of infection with the retargeted Ad5A20TAYT and Ad5A20 mutants in BxPC-3 cells (Fig. 2A) it is possible that the lower EC_{50}-values for both Adwt and mutants masked small differences in cell killing ability in these cells.

Viral genome amplification is increased with A20FMDV2-expressing mutants in cells expressing high levels of the αvß6-integrin.

In Suit-2 and Panc04.03 cells, the enhanced infection and cell killing with the A20FMDV2-mutants were paralleled by higher levels of viral genome amplification compared to infection with Ad5wt at all time points (24-72h) (Fig. 2D). In agreement with the cell killing and infectivity data, Ad5wt genome amplification was greater in PT45 cells with a similar trend in MiaPaCa-2 cell. In BxPC-3 cells, all three viruses replicated to similar levels. In conclusion, variations in the absolute levels of genome amplification between Ad5wt and the retargeted mutants directly reflected the different levels of viral uptake (24h time point) for each cell line as a consequence of the increased number of viral genomes available after infection. In contrast, the relative replication rates of the retargeted mutants in individual cell lines remained similar to Ad5wt.

Blocking αvß6-integrin attenuates infection with Ad5A20 and Ad5A20-477dlTAYT but not with Ad5wt.

The αvß3- and αvß5-integrins play a major role in internalisation of Ad5wt, mediated by penton-integrin binding through RGD-interactions. To examine whether these integrins were also essential for the FMDV-retargeted mutants or whether binding to the αvß6-integrin alone was sufficient for cellular uptake of virus, we first determined the expression levels of αvß3- and αvß5-integrins (Fig 3A). PT45 and Suit2 cells expressed the highest levels of αvß5-integrins and BxPC-3 of the αvß3-integrin. The greatest expression of αvß6-integrins was observed in Suit-2 and Panc04.03 cells. Blocking of αvß6-integrin receptors with free A20FMDV2 peptide significantly decreased the infection levels with Ad5A20 and Ad5A20-477*dl*TAYT but not with Ad5wt in Panc04.03, Suit-2 and BxPC-3 cells (Fig. 3B). The most pronounced effect was in Suit-2 and Panc04.03 cells with reductions up to 70% compared to original

levels of infection. Decreased E1A-expression in cells infected with Ad5A20-477*dl*TAYT but not with Ad5wt further confirmed our findings (Panc0403; Supplementary Fig. 1E). Thus, Ad5A20 and Ad5A20-477*dl*TAYT were mainly internalised through αvß6-integrins in pancreatic cancer cells although, other integrins such as αvß5 may contribute towards the process. Importantly, in cells with low or non-detectable levels of αvß6-integrins, infection with the retargeted mutants was reduced compared to infection with Ad5wt (Fig. 3A-B and Fig. 1B).

Viral replication and spread is supported in organotypic 3-dimensional (3D) co-cultures of pancreatic cancer and stromal cells.

Pancreatic cancer cells (PDAC) *in situ* are typically embedded in a dense tumour-supporting fibrous stroma, with pancreatic stellate cells as a major component promoting invasion and restricting delivery of drugs to the tumour (35, 36). To explore efficacy of the Ad5A20 and Ad5A20-477*dl*TAYT mutants under conditions that are more similar to the tumour micro-environment than 2-dimensional monocultures, Panc04.03 or Suit-2 cells were co-cultured with transformed non-tumorigenic pancreatic stellate cells (PS1) in 3-dimensional (3D) collagen-matrigels (27-29). Growth of both cancer cell lines were greatly increased in the presence of PS1 cells, forming duct-like structures when seeded and cultured within the gels (Supplementary Fig. 2), as previously reported for organoids established from human and murine pancreatic tumour tissue (37-39). Panc04.03 or Suit-2 cells seeded together with PS1 cells on top of gel matrices formed thick epithelial layers with increased cellular invasion into the substrate (Fig. 4Aii; top panels). However, in the absence of PS1 cells, the cancer cells mostly formed monolayers on top of the gels and did not invade the matrices (Fig. 4Ai). The 3D-culture conditions were compatible with adenoviral propagation regardless of where the cells were seeded (Fig. 4A and Supplementary Fig. 2). After 4 days of co-culturing PS1 cells with Panc04.03 or Suit-2 cells, the addition of Ad5wt and Ad5A20 resulted in viral spread through multiple cell layers when cells were seeded on top of the gels. The thickness of the uppermost epithelial layers decreased with increased viral dose, demonstrating virus-dependent cell killing (Fig. 4A; middle and bottom panels). The cell killing was greatest with the Ad5A20 mutant in Panc04.03 cells with few remaining live E1A-positive cells 4 days after infection (Fig. 4A; confocal images). The effect was similar

in Suit-2 cells although, the inhibition of invasion and growth was less than in Panc04.03 cells (Fig. 4A; right panels). Importantly, we demonstrate that the infected epithelial cells were in sufficiently close contact with the PS1 stromal cells for virus to spread through the matrix and infect both cancer and stromal cells (Fig. 4B).

Viral infection and replication in PS1 cells were initially determined in 2-dimensional monocultures (Fig. 4C). As expected for non-epithelial cells the level of infection was poor with the highest levels for Ad5wt with <10% of cells expressing EGFP, and <5% for the retargeted mutants compared to 20-50% in αvß6-integrin-expressing epithelial cancer cells (Fig. 4C and 3B). Importantly, the early viral E1A gene was expressed at detectable levels in the PS1 monolayers (Supplementary Figure 3A-B). Viral uptake was likely mediated by αvß3- and αvß5-integrins (Fig. 4D), and was significantly reduced in the presence of an anti-αvß5-integrin antibody (Fig 4C). CAR and the αvß6-integrin were not detected in PS1 cells (Fig. 4D). We tested whether viruses could be released from infected PS1 cells and spread to neighbouring cancer cells. After infecting PS1 cells with Adwt or Ad5A20, following a 72h incubation period, the cell-free culture media was transferred to Panc04.03 and Suit-2 monocultures. Potent viral infection and early gene expression was observed in both cancer cell lines (shown for Panc04.03; Fig. 4E). Viral spread was also confirmed in 3D cultures by a similar two-step process; PS1 cells pre-seeded onto matrices were infected with viruses and after removal of excess free virus (48h post infection), non-infected Panc04.03 or Suit-2 cells were seeded on top. Sufficient virions were produced from the PS1 cells to infect and eliminate the majority of the cancer cells 72h post-infection (Fig. 4F). These findings collectively provide evidence that the retargeted adenoviral mutants infected both pancreatic stellate and cancer cells and could spread from cell-to-cell in the 3D culture system that represents the tumour microenvironment more accurately.

The novel retargeted and replication-selective oncolytic mutant Ad5-3Δ-A20T is highly efficacious in pancreatic cancer cell lines.

To further exploit the selective targeting to αvß6-integrins on pancreatic cancer cells, the A20FMDV2 peptide was inserted and CAR-binding was ablated in the fibre knob (HI-loop) of the AdΔΔ mutant, to generate Ad5-3Δ-A20T (Fig. 5A and Supplementary Fig. 1B) (6, 23, 24). In addition to the E1ACR2 and E1B19K

deletions in AdΔΔ that provide replication-selectivity and apoptosis-enhancement, deletion of the TAYT-motif and the point-mutation at Y477A were included to reduce CAR-binding. These mutations and the insertion of the A20FMDV2 peptide were identical to the alterations in the parental Ad5A20-477*dl*TAYT mutant (18, 24, 40) (Fig. 5A and Supplementary Fig. 1B). The resulting oncolytic mutant Ad5-3Δ-A20T killed Panc04.03 and Suit-2 cells more potently than the parental AdΔΔ mutant demonstrated by 10- and 5-fold lower EC_{50}-values (Fig. 5B; left panel). In contrast, in PS1 cells that were significantly less sensitive to virus-induced cell killing (>10-fold higher EC_{50}-values), the novel mutant had similar cell killing potency as Ad5wt (Fig. 5B; right panel). Replication of Ad5-3Δ-A20T in Panc04.03 and Suit-2 cells was slightly less than for AdΔΔ (Fig. 5C). Replication in PS1 cells was also less for Ad5-3Δ-A20T than for AdΔΔ. However, both viruses showed >100-fold lower levels of replication in PS1 than in epithelial cells; Ad5-3Δ-A20T replication was $4.2x10^5\pm$ $2.2x10^5$ pfu/ml and AdΔΔ $1.7x10^7\pm$ $5.1x10^6$ pfu/ml (n=3) 48h post-infection in the stromal cells.

Ad5-3Δ-A20T potently inhibits growth and invasion of Panc0403 cells in 3D co-cultures with the pancreatic stromal PS1 cells.

Dose-dependent cell killing was observed when 3D co-cultures of Panc04.03-PS1 cells were infected with Ad5-3Δ-A20T or AdΔΔ (500 and 1000ppc) for 4 days (Panc04.03; Fig. 5D). In cultures infected with Ad5-3Δ-A20T, viable and/or invading cells appeared to be fewer than in AdΔΔ-infected cultures at the lower dose, while the higher dose eliminated most cells with both viruses. Importantly, the efficacy of Ad5-3Δ-A20T was retained in organotypic co-cultures of Panc04.03 or Suit-2 with PS1 cells when treated simultaneously with gemcitabine (Suit-2; Fig. 5E and Supplementary Fig. 4). We previously demonstrated that both AdΔΔ and AdΔ19K synergised with low doses of gemcitabine in pancreatic cancer cells in 2D monocultures and *in vivo*, including Suit-2 models, by enhancing apoptotic death through mitotic aberrations (11, 14). We found that the 3D co-culture system was a suitable model for screening the efficacy of adenoviral mutants and for confirming compatibility with current therapeutic cytotoxic drugs.

Ad5-3Δ-A20T efficiently inhibits growth of human pancreatic cancer xenografts in murine models.

The potent elimination of Panc04.03 and Suit-2 cells grown in 2D mono- and 3D co-cultures were confirmed *in vivo*, using Suit-2 xenografts grown subcutaneously in athymic mice. We have previously demonstrated that the Suit-2 model is suitable for determining efficacy of adenoviral mutants administered alone or in combination with cytotoxic drugs (12, 41). Both Adwt and Ad5-3Δ-A20T potently prevented tumor growth up to 20 days after the first administration of virus (Fig. 6A). From 20-42d growth was greatly reduced compared to the mock-treated animals that were culled already after 18 days due to tumour burden and ulcer formation. The median time to tumor progression was significantly prolonged ($p<0.0004$) from 11d for mock-treated animals to 42d with Ad5-3Δ-A20T and 37d for Adwt (Fig. 6B). Tumours harvested when animals were culled showed intense E1A expression for both viruses up to 53d after virus-administration (Fig. 6C). The ultimate goal of generating Ad5-3Δ-A20T was to increase viral dose at tumour lesions after systemic delivery. In this proof-of-concept study, potent expression of E1A was observed in Suit-2 tumours after a single tail vein administration of Ad5-3Δ-A20T (Fig. 6D). Interestingly, E1A expression appeared to be lower after tail vein injection with Adwt. The results from the 3D co-cultures and the *in vivo* studies demonstrated that Ad5-3Δ-A20T was at least as efficacious as Ad5wt under conditions that more realistically mimic the tumour microenvironment *in situ* in patients. Future studies will be aimed at quantifying the retargeting efficacy in murine models that can mimic the conditions in patients more accurately including systems with humanised blood factors. Taken together our data support further exploration of Ad5-3Δ-A20T for potential future development into novel anti-cancer agents targeting pancreatic cancer.

Discussion

No curative treatments are currently available for patients with metastatic PDAC, and resistance to chemotherapeutics inevitably develops. The recent identification of several biomarkers will hopefully enable earlier detection and curative surgery in more patients (42, 43). In contrast, replication-selective oncolytic adenoviral mutants target pancreatic cancer at any stage by direct oncolysis, reversal of drug resistance and activation of anti-tumour immune responses but have poor efficacy when delivered systemically (8, 10). The focus of our study was to optimize the potent and selective oncolytic mutant AdΔΔ (6) to enable future development of this mutant for systemic delivery by taking advantage of the selective expression of αvß6-integrin in

pancreatic cancer cells. We generated the replication-selective integrin-targeted Ad5-3Δ-A20T mutant expressing the small αvß6-peptide ligand A20FMDV2. The A20FMDV2 peptide was derived from the GH-loop in VP1 in the capsid of the foot-and-mouth disease virus (FMDV) and is essential for infection in cloven-hoofed animals (44). The affinity to αvß6-integrins was high, measured at K_D=0.22nM, while binding to other integrins, including αvß3, αvß5 and αvß1 was more than 80-fold lower (21, 25). The selective binding to αvß6-integrins was shown to be dependent on the DLXXL motif in the carboxy α-helical loop next to the RGD-domain at the apex of the loop domain in the peptide (23, 26, 44, 45).

We previously demonstrated that the retargeted wild type mutants Ad5A20 and Ad5A20-477*dl*TAYT infected breast and ovarian carcinoma cells expressing the αvß6-integrin (23, 24). In the current study, we demonstrated that infection with these mutants strongly correlated with αvß6-integrin levels in a panel of fifteen PDAC cell lines. In two cell lines that express relatively high levels of αvß6-integrins (CFPAC-1 and Capan-2), lower than expected levels of infection with the retargeted mutants were observed. In the same cell lines, lower infection levels were demonstrated with Ad5wt which overall suggest that these cells are generally insensitive to viral infection and/or viral gene expression. Correspondingly, transduction of CFPAC-1 cells with native Ad5, expressing a reporter gene, was demonstrated to be less efficient than of MIA PaCa-2, PANC-1 and BxPC-3 cells (46). Infectivity was monitored by viral EGFP expression, which in turn was regulated by the early viral E1A gene product, suggesting that both retargeted mutants entered the early endosomes even when attachment was through the αvß6-integrin rather than CAR. The classical route of internalization of native Ad5 is via fibre knob-binding to CAR on epithelial cells, which initiates binding of penton base proteins to αvß3- and αvß5-integrins through RGD-motifs, activating clathrin-mediated endocytosis (47). Acidification of the virus-containing endosome is required for release of viral genomes and proteins into the cytosol and for transport into the nucleus and completion of the viral life cycle. The level of infection by the retargeted mutants correlated with expression levels of the αvß6-integrins and was reflected in the degree of cell killing in all the selected cell lines except BxPC-3. This cell line expressed all the tested integrins (αvß3-, αvß5-, and αvß6) and CAR. The presence of these receptors likely contributed to the high sensitivity to Adwt infection producing the

lowest EC_{50}-values of all tested cell lines allowing for only small differences in cell killing ability between Adwt and the retargeted mutants. It is interesting to note that both Panc04.03 and Suit-2 have low levels of CAR and the αvß3-integrin and the highest levels of αvß6-integrin expression, the reverse of the BxPC-3 cells.

To further support the notion that our retargeted mutants likely internalise and infect in a similar way to wild type virus, we showed that total viral genome amplification paralleled the levels of infectivity, whereas the rate of replication remained similar to that of Ad5wt in each cell line. Thus, viral propagation was not hampered by the retargeted fibers and nuclear entry of the viral genome could proceed. Internalisation of the re-targeted mutants via αvß6-integrin was confirmed by blocking infection with free A20FMDV2 peptide. Intracellular processing of the FMDV virus is less established, but includes a pathway similar to that of Ad5, with additional intracellular mechanisms implicated (48). It was recently reported that binding of the A20FMDV2 peptide alone to normal human bronchial epithelial (NHBE) cells caused rapid internalization of the peptide-αvß6-integrin complex in endosomes although, the post-internalisation events were suggested to be more complex with partial delay of recycling of the integrin to the cell surface (25). Nevertheless, our αvß6-integrin retargeted Ad5 mutants infected and replicated to similar levels as Adwt in PDAC cells. The exact cellular factors involved in the internalization, endocytosis, nuclear transport or the rate of cellular processing, may differ for viruses internalized via αvß6- compared to αvß3- and αvß5-integrins. Interestingly, pancreatic stellate cells that lack αvß6-integrins were infected by Ad5-3Δ-A20T, suggesting that uptake in these cells was dependent on other integrins including αvß5, in the presence of high local doses of virus. These processes are the subjects for future investigations.

Following the initial proof-of concept studies, the chimeric fiber from Ad5A20-477*dl*TAYT was engineered into the AdΔΔ mutant to generate Ad5-3Δ-A20T. The additional modifications to the CAR-binding region of the fibre-knob were also retained as a strategy to facilitate systemic delivery in future studies. We previously found that Ad5A20-477*dl*TAYT had improved liver-to-tumour viral genome ratios possibly through abrogation of FIX/C4BP-binding due to the TAYT-deletion (18, 24). Importantly, Ad5A20-477*dl*TAYT did not agglutinate erythrocytes due to de-targeting of CAR through the Y477A mutation. The novel Ad5-3Δ-A20T mutant infected and killed αvß6-integrin expressing PDAC cells more efficiently than both

Ad5wt and the parental AdΔΔ mutant. Viral functions including infection, gene expression and viral replication were retained, supporting propagation in all tested cell lines. However, replication was slightly lower with the new mutant than with AdΔΔ, indicating that the increased viral uptake and consequently, early viral gene expression, initiated cell killing before maximal number of virions were produced, as previously demonstrated in NHBE cells and PDAC cells treated with viral replication-inhibitors (12). Furthermore, Ad5-3Δ-A20T had approximately a 4-fold higher vp/pfu ratio compared to Adwt or AdΔΔ although, production in A549 cells resulted in similar yields of viral particles for all three viruses. Nevertheless, Ad5-3Δ-A20T was as potent as Ad5wt in tumour xenograft models in athymic mice. When injected intratumourally the retargeted mutant spread within the solid tumours similar to Ad5wt and as previously reported for AdΔΔ (6). Complete elimination of tumours was not possible with either Ad5-3Δ-A20T or Ad5wt because of limitations of the *in vivo* model. Murine tissues do not support productive infection with human adenovirus, preventing spread within the murine tumour microenvironment in addition to the rapid xenograft growth and the absence of an immune response (49). Despite the rapid hepatic elimination of adenovirus in mice, we confirmed that intravenous delivery of Ad5-3Δ-A20T resulted in high levels of viral gene expression in Suit-2 tumours. Future studies will address whether the retargeted mutant will reach tumours in sufficiently high levels to warrant systemic administration. Importantly, the Suit-2 cells employed in the xenograft studies expressed lower levels of αvß6-integrin and higher levels of αvß5 compared to Panc04.03 cells. We predict that tumour xenografts with similar integrin-profiles, high αvß6- and lower αvß3- and αvß5-integrin expression, would reflect the higher cell killing seen *in vitro*.

We optimised the previously developed 3D co-culture models of pancreatic stellate and cancer cell lines (27-29), for investigating viral infection and spread in this study. These models have more similarities with the tumour microenvironment in patients than traditional 2D monocultures. In addition, the interaction with human stromal cells is retained without interference from murine stroma present in athymic mice models. Although, more sophisticated organoid culture models have been described for murine and patient tumour tissue including a few methods for modeling pancreatic cancer (37, 39), we found that our 3D co-cultures were more suitable for screening of viral functions. We found that both Ad5-3Δ-A20T and Ad5A20 were more

efficacious than Ad5wt and AdΔΔ in infecting and eliminating Panc04.03 and Suit-2 cells while in the murine models the novel retargeted Ad5-3Δ-A20T had similar efficacy to Adwt. The collagen-matrigel matrices are likely to provide a more penetrable milieu for viral infectivity and spread than in dense murine stroma further facilitating the enhanced infectivity of Ad5-3Δ-A20T as demonstrated in the 2D cultures. We showed that human stellate cells (PS1) support viral infection and replication, albeit at significantly lower levels than pancreatic cancer cells, which could further augment viral spread within the cultures, in contrast to the murine test model. Our data demonstrate that viral efficacy was retained in the 3D-cultures when Ad5-3Δ-A20T was combined with low doses of gemcitabine. The deletion of the E1B19K gene causes enhancement of gemcitabine-dependent apoptosis, previously demonstrated for AdΔΔ in PDAC cells (6, 11, 12, 14). We propose that the 3D co-cultures are suitable model systems for investigating oncolytic virus replication and spread in the presence of the multiple cell types that constitute the tumour microenvironment in patients. The flexibility of the system is achieved by varying the cell and matrix compositions; and treatment with viruses and/or drugs can be administered via different compartments to enable a tailored test system appropriate for the research question. In conclusion, the 3D cultures complement the limitations of 2D cell cultures and murine *in vivo* models by providing a suitable platform for selecting the best viral mutant candidates to pursue clinically.

Herein, we provide evidence that the complex alterations of the viral genome in the novel selective Ad5-3Δ-A20T mutant did not compromise viral functions in αvß6-integrin expressing PDAC cells but rather enhanced infectivity and cell killing selectively, in these cells. In addition to the E1ACR2 and E1B19K deletions for replication-selectivity and apoptosis-enhancement in AdΔΔ, the E3gp19K gene was deleted to increase recruitment of immune cells to infected tumour cells with the aim to enhance efficacy in future clinical applications. We consider Ad5-3Δ-A20T an excellent candidate for targeting pancreatic cancer. Further bio-distribution studies will elucidate whether additional modifications are necessary to eliminate tumours after systemic delivery, for example, by introducing modifications to avoid neutralizing antibodies and/or hepatic elimination. Our results may open new avenues for improving the delivery and efficacy of potent oncolytic adenoviral mutants in patients with pancreatic cancer.

Acknowledgements

This study was supported by generous grants from the UK Charity Pancreatic Cancer Research Fund (PCRF) and the BCI CRUK Centre Grant [grant number C16420/A18066] (G. Halldén, S. Man, C. Pantelidou), and the CRUK Biotherapeutics Drug Discovery Project Award [grant number 23946] (A. Parker, J. Davies). We want to thank Dr Elisabete Carapuca for expert suggestions on IHC and confocal microscopy, and Professor Hemant Kocher for the kind gift of PS1 cells and helpful discussions and advice. We greatly appreciate the excellent assistance by Julie Andow, Tracy Chaplin-Perkins and Hagen Schmidt.

References

1. Oettle H. Progress in the knowledge and treatment of advanced pancreatic cancer: from benchside to bedside. Cancer treatment reviews. 2014;40:1039-47.
2. Kulke MH, Tempero MA, Niedzwiecki D, Hollis DR, Kindler HL, Cusnir M, et al. Randomized phase II study of gemcitabine administered at a fixed dose rate or in combination with cisplatin, docetaxel, or irinotecan in patients with metastatic pancreatic cancer: CALGB 89904. J Clin Oncol. 2009;27:5506-12.
3. Hecht JR, Bedford R, Abbruzzese JL, Lahoti S, Reid TR, Soetikno RM, et al. A phase I/II trial of intratumoral endoscopic ultrasound injection of ONYX-015 with intravenous gemcitabine in unresectable pancreatic carcinoma. Clin Cancer Res. 2003;9:555-61.
4. Mulvihill S, Warren R, Venook A, Adler A, Randlev B, Heise C, et al. Safety and feasibility of injection with an E1B-55 kDa gene-deleted, replication-selective adenovirus (ONYX-015) into primary carcinomas of the pancreas: a phase I trial. Gene Ther. 2001;8:308-15.
5. O'Shea CC, Johnson L, Bagus B, Choi S, Nicholas C, Shen A, et al. Late viral RNA export, rather than p53 inactivation, determines ONYX-015 tumor selectivity. Cancer Cell. 2004;6:611-23.
6. Öberg D, Yanover E, Sweeney K, Adam V, Costas C, Lemoine NR, et al. Improved potency and selectivity of an oncolytic E1ACR2 and E1B19K deleted adenoviral mutant (AdΔΔ) in prostate and pancreatic cancers. Clin Cancer Res. 2010:541-53.
7. Raki M, Kanerva A, Ristimaki A, Desmond RA, Chen DT, Ranki T, et al. Combination of gemcitabine and Ad5/3-Delta24, a tropism modified conditionally replicating adenovirus, for the treatment of ovarian cancer. Gene Ther. 2005;12:1198-205.
8. Jiang H, Clise-Dwyer K, Ruisaard KE, Fan X, Tian W, Gumin J, et al. Delta-24-RGD oncolytic adenovirus elicits anti-glioma immunity in an immunocompetent mouse model. PLoS One. 2014;9:e97407.
9. Jones S, Zhang X, Parsons DW, Lin JC, Leary RJ, Angenendt P, et al. Core signaling pathways in human pancreatic cancers revealed by global genomic analyses. Science. 2008;321:1801-6.
10. Martinez-Velez N, Xipell E, Jauregui P, Zalacain M, Marrodan L, Zandueta C, et al. The oncolytic adenovirus Delta24-RGD in combination with cisplatin exerts a potent anti-osteosarcoma activity. Journal of bone and mineral research. 2014;29:2287-96.
11. Cherubini G, Kallin C, Mozetic A, Hammaren-Busch K, Muller H, Lemoine NR, et al. The oncolytic adenovirus AdDeltaDelta enhances selective cancer cell killing in combination with DNA-damaging drugs in pancreatic cancer models. Gene Ther. 2011;18:1157-65.
12. Leitner S, Sweeney K, Oberg D, Davies D, Miranda E, Lemoine NR, et al. Oncolytic adenoviral mutants with E1B19K gene deletions enhance gemcitabine-induced apoptosis in pancreatic carcinoma cells and anti-tumor efficacy in vivo. Clin Cancer Res. 2009;15:1730-40.
13. White E. Mechanisms of apoptosis regulation by viral oncogenes in infection and tumorigenesis. Cell Death Differ. 2006;13:1371-7.
14. Pantelidou C, Cherubini G, Lemoine NR, Hallden G. The E1B19K-deleted oncolytic adenovirus mutant AdDelta19K sensitizes pancreatic cancer cells to

drug-induced DNA-damage by down-regulating Claspin and Mre11. Oncotarget. 2016;7:15703-24.
15. Carlisle RC, Di Y, Cerny AM, Sonnen AF, Sim RB, Green NK, et al. Human erythrocytes bind and inactivate type 5 adenovirus by presenting Coxsackie virus-adenovirus receptor and complement receptor 1. Blood. 2009;113:1909-18.
16. Jonsson MI, Lenman AE, Frangsmyr L, Nyberg C, Abdullahi M, Arnberg N. Coagulation factors IX and X enhance binding and infection of adenovirus types 5 and 31 in human epithelial cells. J Virol. 2009;83:3816-25.
17. Kalyuzhniy O, Di Paolo NC, Silvestry M, Hofherr SE, Barry MA, Stewart PL, et al. Adenovirus serotype 5 hexon is critical for virus infection of hepatocytes in vivo. Proceedings of the National Academy of Sciences of the United States of America. 2008;105:5483-8.
18. Shayakhmetov DM, Gaggar A, Ni S, Li ZY, Lieber A. Adenovirus binding to blood factors results in liver cell infection and hepatotoxicity. J Virol. 2005;79:7478-91.
19. Doronin K, Flatt JW, Di Paolo NC, Khare R, Kalyuzhniy O, Acchione M, et al. Coagulation factor X activates innate immunity to human species C adenovirus. Science. 2012;338:795-8.
20. Bates RC, Bellovin DI, Brown C, Maynard E, Wu B, Kawakatsu H, et al. Transcriptional activation of integrin beta6 during the epithelial-mesenchymal transition defines a novel prognostic indicator of aggressive colon carcinoma. The Journal of clinical investigation. 2005;115:339-47.
21. Hausner SH, Abbey CK, Bold RJ, Gagnon MK, Marik J, Marshall JF, et al. Targeted in vivo imaging of integrin alphavbeta6 with an improved radiotracer and its relevance in a pancreatic tumor model. Cancer Res. 2009;69:5843-50.
22. Allen MD, Thomas GJ, Clark S, Dawoud MM, Vallath S, Payne SJ, et al. Altered microenvironment promotes progression of preinvasive breast cancer: myoepithelial expression of alphavbeta6 integrin in DCIS identifies high-risk patients and predicts recurrence. Clin Cancer Res. 2014;20:344-57.
23. Coughlan L, Vallath S, Saha A, Flak M, McNeish IA, Vassaux G, et al. In vivo retargeting of adenovirus type 5 to alphavbeta6 integrin results in reduced hepatotoxicity and improved tumor uptake following systemic delivery. J Virol. 2009;83:6416-28.
24. Coughlan L, Vallath S, Gros A, Gimenez-Alejandre M, Van Rooijen N, Thomas GJ, et al. Combined fiber modifications both to target alpha(v)beta(6) and detarget the coxsackievirus-adenovirus receptor improve virus toxicity profiles in vivo but fail to improve antitumoral efficacy relative to adenovirus serotype 5. Hum Gene Ther. 2012;23:960-79.
25. Slack RJ, Hafeji M, Rogers R, Ludbrook SB, Marshall JF, Flint DJ, et al. Pharmacological Characterization of the alphavbeta6 Integrin Binding and Internalization Kinetics of the Foot-and-Mouth Disease Virus Derived Peptide A20FMDV2. Pharmacology. 2016;97:114-25.
26. Dicara D, Burman A, Clark S, Berryman S, Howard MJ, Hart IR, et al. Foot-and-mouth disease virus forms a highly stable, EDTA-resistant complex with its principal receptor, integrin alphavbeta6: implications for infectiousness. J Virol. 2008;82:1537-46.
27. Froeling FE, Mirza TA, Feakins RM, Seedhar A, Elia G, Hart IR, et al. Organotypic culture model of pancreatic cancer demonstrates that stromal cells modulate E-cadherin, beta-catenin, and Ezrin expression in tumor cells. The American journal of pathology. 2009;175:636-48.

28. Coleman SJ, Chioni AM, Ghallab M, Anderson RK, Lemoine NR, Kocher HM, et al. Nuclear translocation of FGFR1 and FGF2 in pancreatic stellate cells facilitates pancreatic cancer cell invasion. EMBO molecular medicine. 2014;6:467-81.
29. Carapuca EF, Gemenetzidis E, Feig C, Bapiro TE, Williams MD, Wilson AS, et al. Anti-stromal treatment together with chemotherapy targets multiple signalling pathways in pancreatic adenocarcinoma. The Journal of pathology. 2016;239:286-96.
30. Jackson T, Sheppard D, Denyer M, Blakemore W, King AM. The epithelial integrin alphavbeta6 is a receptor for foot-and-mouth disease virus. J Virol. 2000;74:4949-56.
31. Merron A, Peerlinck I, Martin-Duque P, Burnet J, Quintanilla M, Mather S, et al. SPECT/CT imaging of oncolytic adenovirus propagation in tumours in vivo using the Na/I symporter as a reporter gene. Gene Ther. 2007;14:1731-8.
32. Warming S, Costantino N, Court DL, Jenkins NA, Copeland NG. Simple and highly efficient BAC recombineering using galK selection. Nucleic acids research. 2005;33:e36.
33. Stanton RJ, McSharry BP, Armstrong M, Tomasec P, Wilkinson GW. Re-engineering adenovirus vector systems to enable high-throughput analyses of gene function. BioTechniques. 2008;45:659-62, 64-8.
34. Hezel AF, Deshpande V, Zimmerman SM, Contino G, Alagesan B, O'Dell MR, et al. TGF-beta and alphavbeta6 integrin act in a common pathway to suppress pancreatic cancer progression. Cancer Res. 2012;72:4840-5.
35. Froeling FE, Marshall JF, Kocher HM. Pancreatic cancer organotypic cultures. Journal of biotechnology. 2010;148:16-23.
36. Coleman SJ, Watt J, Arumugam P, Solaini L, Carapuca E, Ghallab M, et al. Pancreatic cancer organotypics: High throughput, preclinical models for pharmacological agent evaluation. World journal of gastroenterology. 2014;20:8471-81.
37. Boj SF, Hwang CI, Baker LA, Chio, II, Engle DD, Corbo V, et al. Organoid models of human and mouse ductal pancreatic cancer. Cell. 2015;160:324-38.
38. Ohlund D, Handly-Santana A, Biffi G, Elyada E, Almeida AS, Ponz-Sarvise M, et al. Distinct populations of inflammatory fibroblasts and myofibroblasts in pancreatic cancer. The Journal of experimental medicine. 2017;214:579-96.
39. Baker LA, Tiriac H, Clevers H, Tuveson DA. Modeling pancreatic cancer with organoids. Trends in cancer. 2016;2:176-90.
40. Kirby I, Davison E, Beavil AJ, Soh CP, Wickham TJ, Roelvink PW, et al. Mutations in the DG loop of adenovirus type 5 fiber knob protein abolish high-affinity binding to its cellular receptor CAR. J Virol. 1999;73:9508-14.
41. Bhattacharyya M, Francis J, Eddouadi A, Lemoine NR, Hallden G. An oncolytic adenovirus defective in pRb-binding (dl922-947) can efficiently eliminate pancreatic cancer cells and tumors in vivo in combination with 5-FU or gemcitabine. Cancer Gene Ther. 2011;18:734-43.
42. Radon TP, Massat NJ, Jones R, Alrawashdeh W, Dumartin L, Ennis D, et al. Identification of a Three-Biomarker Panel in Urine for Early Detection of Pancreatic Adenocarcinoma. Clin Cancer Res. 2015;21:3512-21.
43. Debernardi S, Massat NJ, Radon TP, Sangaralingam A, Banissi A, Ennis DP, et al. Noninvasive urinary miRNA biomarkers for early detection of pancreatic adenocarcinoma. American journal of cancer research. 2015;5:3455-66.

44. Berryman S, Clark S, Kakker NK, Silk R, Seago J, Wadsworth J, et al. Positively charged residues at the five-fold symmetry axis of cell culture-adapted foot-and-mouth disease virus permit novel receptor interactions. J Virol. 2013;87:8735-44.
45. DiCara D, Rapisarda C, Sutcliffe JL, Violette SM, Weinreb PH, Hart IR, et al. Structure-function analysis of Arg-Gly-Asp helix motifs in alpha v beta 6 integrin ligands. The Journal of biological chemistry. 2007;282:9657-65.
46. Bouvet M, Bold RJ, Lee J, Evans DB, Abbruzzese JL, Chiao PJ, et al. Adenovirus-mediated wild-type p53 tumor suppressor gene therapy induces apoptosis and suppresses growth of human pancreatic cancer. Annals of surgical oncology. 1998;5:681-8.
47. Meier O, Greber UF. Adenovirus endocytosis. J Gene Med. 2004;6 Suppl 1:S152-63.
48. Miller LC, Blakemore W, Sheppard D, Atakilit A, King AM, Jackson T. Role of the cytoplasmic domain of the beta-subunit of integrin alpha(v)beta6 in infection by foot-and-mouth disease virus. J Virol. 2001;75:4158-64.
49. Cheong SC, Wang Y, Meng JH, Hill R, Sweeney K, Kirn D, et al. E1A-expressing adenoviral E3B mutants act synergistically with chemotherapeutics in immunocompetent tumor models. Cancer Gene Ther. 2008;15:40-50.

Figure legends

Figure 1. Higher levels of αvβ6-integrin expression in pancreatic cancer cell lines support higher levels of infection with the retargeted A20FMDV2-expressing Ad5A20 and Ad5A20-477*dl*TAYT mutants. A) Fifteen pancreatic epithelial cancer cell lines were screened for expression of αvβ6-integrin and CAR. Cells were probed with αvβ6- or CAR-specific antibodies, detected by flow cytometry and expression presented as Geometric Mean values, one representative study. **B)** Viral infectivity levels in the panel of cells were determined by flow cytometry. Cells were infected with Ad5wt, Ad5A20 and Ad5A20-477*dl*TAYT at 100ppc, assay was performed 48h post-infection and EGFP expression was quantified, one representative study. **C)** Correlation of data from studies performed as in A-B, for αvβ6-integrin expression and degree of infectivity of Ad5A20 (upper panel) and Ad5A20-477*dl*TAYT (lower panel). Viral infectivity is expressed as a ratio of that corresponding to Ad5wt, to isolate the effect on infectivity mediated by the αvβ6-integrin only. R^2 values are displayed following linear regression analysis, one representative study out of three.

Figure 2. The cell killing potency of Ad5A20 and Ad5A20-477*dl*TAYT is significantly higher than that of Ad5wt in αvβ6-integrin expressing pancreatic cancer cell lines. Five pancreatic cell lines spanning low to high expression levels of αvβ6-integrin were selected for further studies. **A)** Cells were infected with Ad5wt, Ad5A20 and Ad5A20-477*dl*TAYT at 100ppc and infectivity quantified by flow cytometry via EGFP detection, 48h post-infection, n≥3. **B)** A strong correlation between αvβ6-integrin expression and Ad5A20/Ad5wt was observed in the five cell lines (R^2=0.99). **C)** For each cell line viral dose-response curves were generated and cell viability was analysed (MTS-assay) 72h post-infection. EC_{50}-values were determined for each virus and normalised to the EC_{50}-value of Ad5wt per cell line. The increasing αvβ6-integrin expression levels are indicated on the graph. A and C, error bars represent SD, n≥3, *p<0.05, **p<0.01, One-way Anova. **D)** Viral DNA replication was quantified by qPCR. Cells were infected (100ppc) with the indicated viral mutant and harvested 24, 48 and 72h later. Results were compared amongst the three viruses by normalising the values to that of Ad5wt at 24 h and are expressed as

fold-change, n≥2, *p<0.01, One-way Anova comparing mutant/Adwt at indicated time points and 72h/24h.

Figure 3. Cellular uptake of Ad5A20 and Ad5A20-477*dl*TAYT is blocked by free A20FMDV2-peptide in cells expressing high levels of αvβ6-integrin. A) Expression profile of the integrin receptors (αvβ3, αvβ5 and αvβ6) was determined in four selected pancreatic cancer cell lines. Relative expression levels were quantified by flow cytometry and represented by the Geo Mean values, n=3. *p<0.001 (αvβ6), °p<0.001 (αvβ5), compared to levels in PT45. **B)** To verify αvβ6-integrin mediated viral infection, the receptor was blocked with the αvβ6-specific peptide (FMDVp; 10nM) prior to viral infection (100ppc), and analysed for EGFP expression 48 h later. n=3, *p<0.02, **p<0.01, t-test, two-tailed.

Figure 4. Efficient cell killing upon delivery of Ad5wt and Ad5A20, in 3-dimensional organotypic cultures consisting of pancreatic cancer and stromal cells (PS1). A) Panc04.03 or Suit-2 cells were seeded on top of a gel matrix consisting of collagen and Matrigel either alone (i) or co-cultured (ii) with PS1 cells. The co-cultured cells were infected at 1000 and 2000ppc 4d after seeding and fixed in formalin 4d after infection, embedded in paraffin, sectioned and stained with H/E, 5x magnification. For confocal imaging, cellular nuclei were detected with DAPI (blue) and antibodies for E1A (green). **B**) Ad5A20 infects both Panc04.03 and PS1 cells. Sections were stained with H/E (upper panels) and for confocal imaging (lower panels). PS1 cells were identified by α-SMA expression (red) and the localisation of virus identified by E1A expression (green). Nuclei were detected with DAPI (blue) 20x magnification. Area demarcated in the yellow square is magnified in the right panel. Infected PS1 cells appear yellow (white arrows). One representative study is shown, n≥3. **C)** Infection of PS1 cells with Adwt, Ad5A20 and Ad5A20-477*dl*TAYT (1000ppc) was challenged by blocking with αvβ5-integrin specific antibody (clone P1F6, 10µg/ml). EGFP positive cells were detected by flow cytometry 72h post infection. **D**) Relative expression levels of cell surface integrins αvβ3, αvβ5, αvβ6, and CAR in PS1 cells, quantified by flow cytometry, n=3. **E)** PS1 cells were infected with Adwt or AdA20 (4000ppc) for 72h, virus-containing cell-free media was prepared, and 50µl was transferred to epithelial 2D monocultures. Panc04.03 cells

were trypsinised 24h later and analysed for EGFP expression by FACS, n=3. **F)** PS1 cells were seeded on top of the gel, 24h later cells were infected with AdA20 (2000ppc; right panels) or mock-treated (left panels). After 48h the cultures were washed to remove non-internalised virus and Panc04.03 (lower panels) or Suit2 (upper panels) cells were seeded on top of gels, 4d later the cultures were fixed and stained for E1A expression (brown) and H/E, 20x magnification. Black arrows indicate non-infected (left panels) and infected (right panels) fibroblasts, white arrows indicate non-infected (left panels) and infected (right panels) epithelial cells, white dashed arrows point towards lysed or necrotic cells.

Figure 5. The novel retargeted oncolytic mutant Ad5-3Δ-A20T potently infects, replicates and kills co-cultured pancreatic cancer and stromal cells with and without gemcitabine. A) Schematic diagram of the modified Ad5-3Δ-A20T derived from the potent and replication-selective oncolytic mutant AdΔΔ, for details see text. **B)** Viral dose-response curves were generated (MTS-assay) to compare cell viability of AdΔΔ against Ad5-3Δ-A20T in Panc04.03 and Suit-2 cells (left panel), and PS1 cells (right panel), 72h post infection. Representative study, n=3. **C)** Viral replication determined by $TCID_{50}$ assay. Cells were infected with Ad5-3Δ-A20T or AdΔΔ (100ppc) for 48 and 72h and virus collected from media and cells and applied on JH293 cells for replication assay, n=2. **D**) Panc04.03 cells co-cultured with PS1 cells in 3D collagen/matrigels. After 4 days, Ad5-3Δ-A20T was applied (top panel;500-1000ppc) or AdΔΔ (lower panel; 500-1000ppc) in serum free media from the top of the cultures, harvested 4 days after infection and stained with H/E, 5x magnification. **E)** Suit-2 cells co-cultured with PS1 cells as above and 4 days after seeding infected with Ad-3Δ-A20T at the indicated doses ± gemcitabine at 5nM, representative images, n=3. Cultures were harvested 4 days after infection and stained with H/E. Lower panels; confocal images of the corresponding sections stained for DAPI (blue; nuclei) and E1A (green).

Figure 6. Ad5-3Δ-A20T inhibits growth of Suit-2 tumour xenografts in athymic mice. A) Suit-2 cells ($1x10^6$ cells) were inoculated subcutaneously in one flank of CD*nu/nu* athymic mice. Adenoviral mutants or PBS (mock controls) were administrated intra-tumourally ($3x10^9$vp/injection) on day 1, 3 and 6 (arrows), when tumours had reached 100±20µl (14 days after inoculation). Tumor growth was

determined until tumors reached 1.44cm^2. One-way Anova, ***p<0.001 compared to mock, 8 animals/group. **B)** Kaplan Meyer survival curves generated from time to tumour progression set at 500µl. **p<0.01 compared to mock, n=8. **C)** Tissue sections from tumours harvested at the end of the study, stained for E1A expression by IHC, representative tumour images (5x and 20x magnification as shown). **D)** Detection of E1A viral protein in Suit-2 tumour lysates from animals administered a single tail vein injection (3x10^{9}vp/100µl) with the respective virus. Animals were treated when tumour volumes reached 120 ± 30mm^3 in size. Tumours were excised and sonicated 72h later for immunoblotting analysis, one representative study from two animals, 20µg total protein/lane.

Figure 1

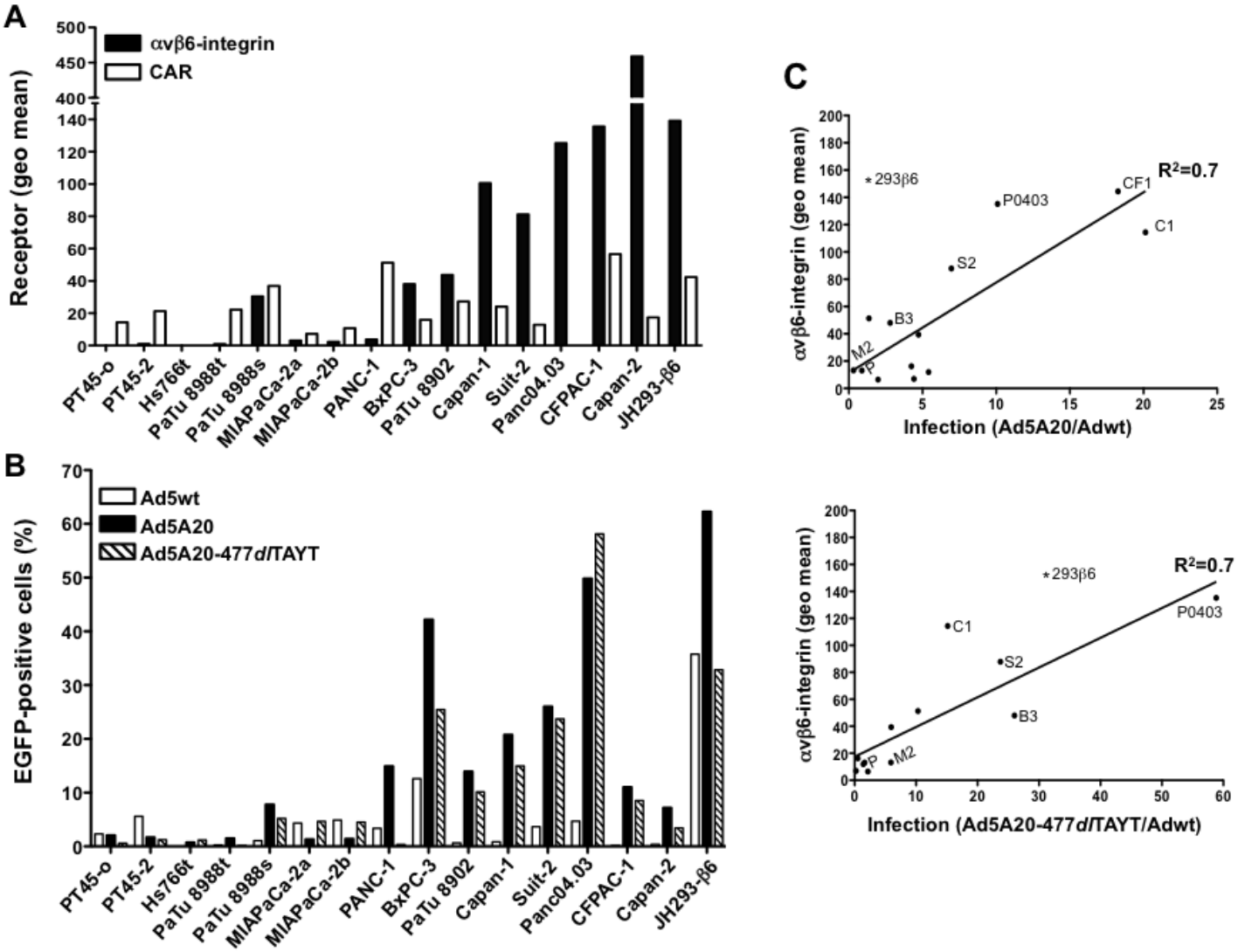
A
αvβ6-integrin
CAR
Receptor (geo mean)
PT45-o
PT45-2
Hs766t
PaTu 8988t
PaTu 8988s
MIAPaCa-2a
MIAPaCa-2b
PANC-1
BxPC-3
PaTu 8902
Capan-1
Suit-2
Panc04.03
CFPAC-1
Capan-2
JH293-β6
B
Ad5wt
Ad5A20
Ad5A20-477dITAYT
EGFP-positive cells (%)
C
αvβ6-integrin (geo mean)
293β6
P0403
CF1
C1
S2
B3
M2
P
R²=0.7
Infection (Ad5A20/Adwt)
Infection (Ad5A20-477dITAYT/Adwt)

Figure 2

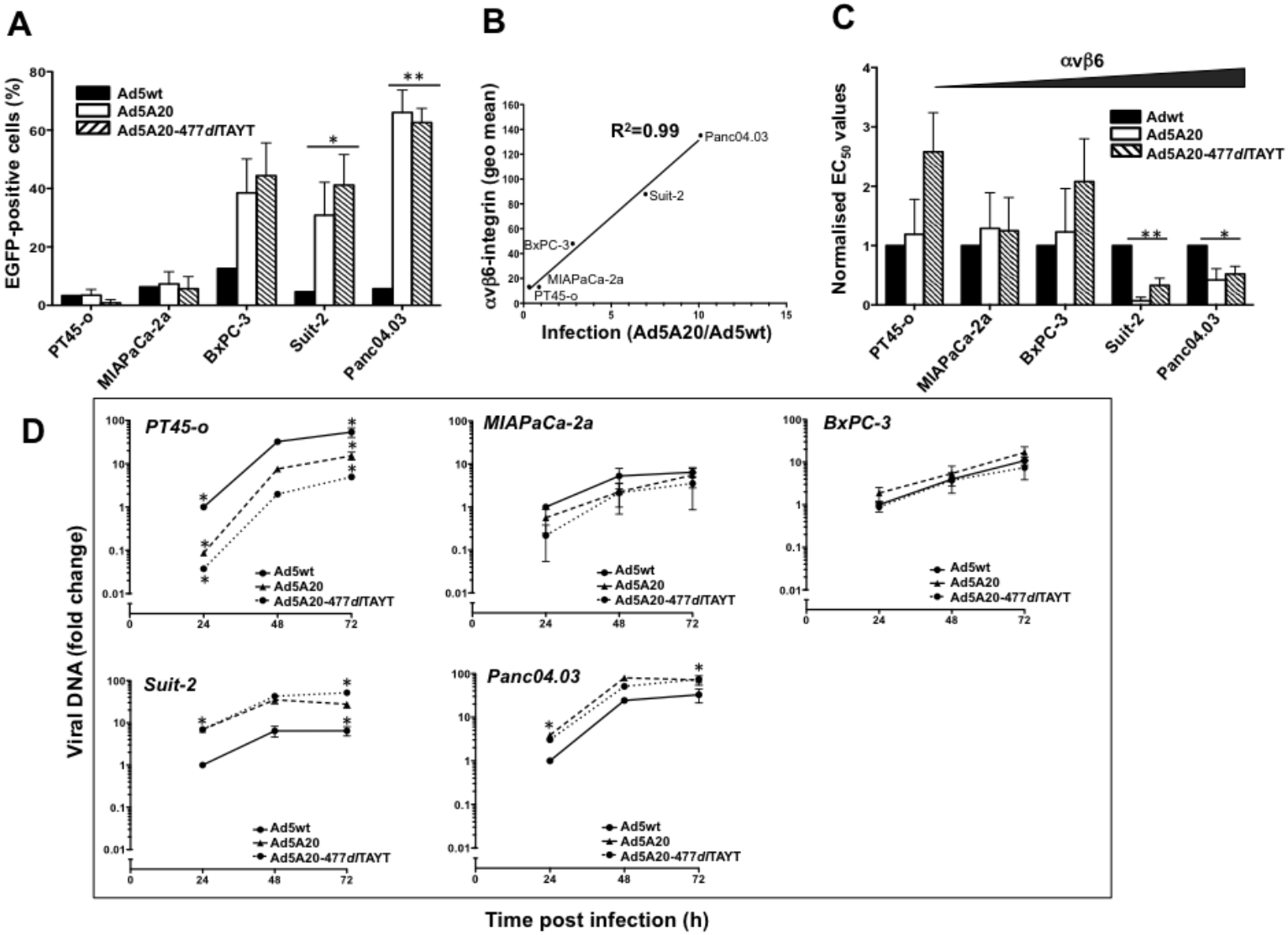
A
EGFP-positive cells (%)
Ad5wt
Ad5A20
Ad5A20-477dlTAYT
PT45-o
MIAPaCa-2a
BxPC-3
Suit-2
Panc04.03
B
αvβ6-integrin (geo mean)
R²=0.99
Infection (Ad5A20/Ad5wt)
C
αvβ6
Normalised EC50 values
Adwt
D
Viral DNA (fold change)
Time post infection (h)

Figure 3

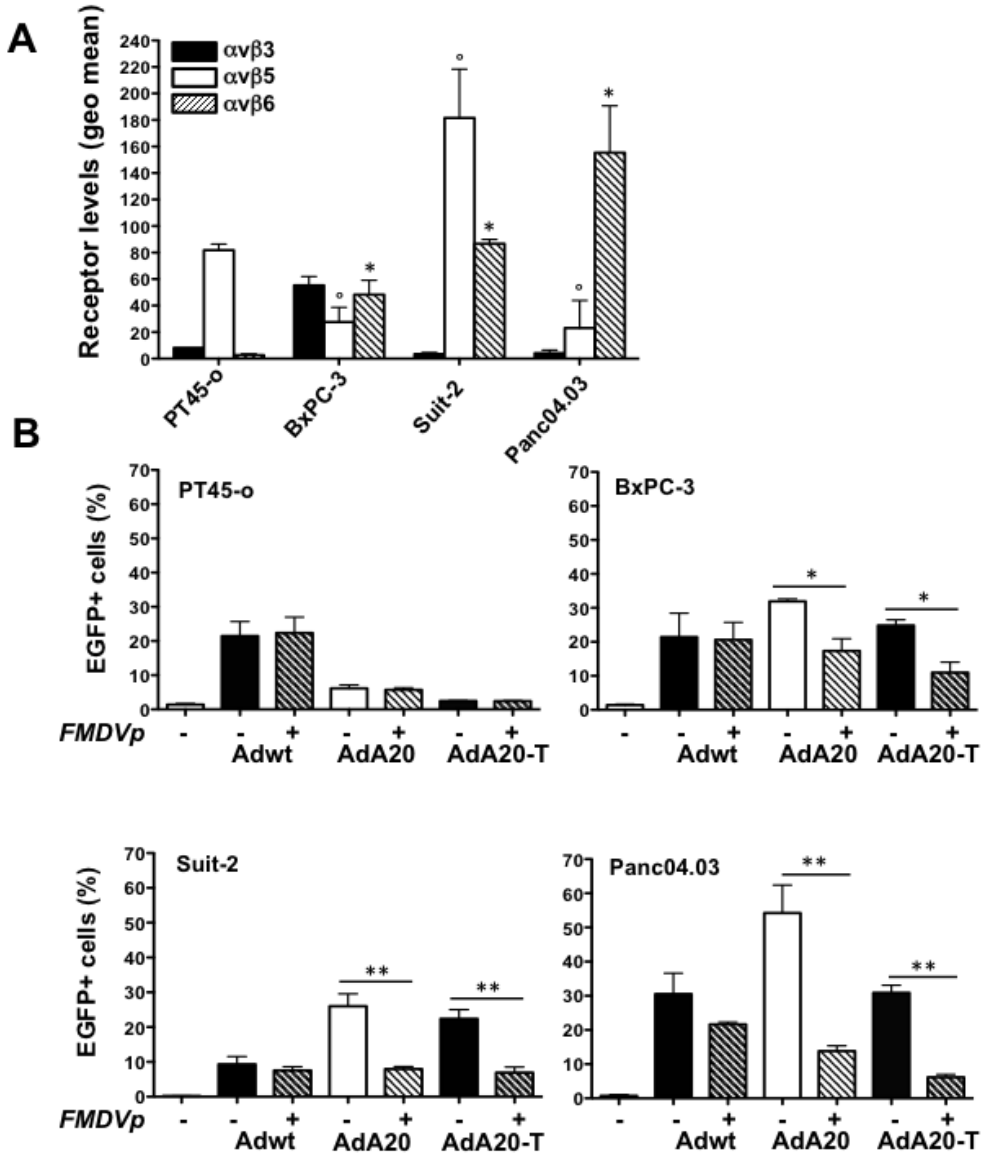
A
Receptor levels (geo mean)
αvβ3
αvβ5
αvβ6
PT45-o
BxPC-3
Suit-2
Panc04.03
B
EGFP+ cells (%)
PT45-o
BxPC-3
Suit-2
Panc04.03
FMDVp
Adwt
AdA20
AdA20-T

Figure 4

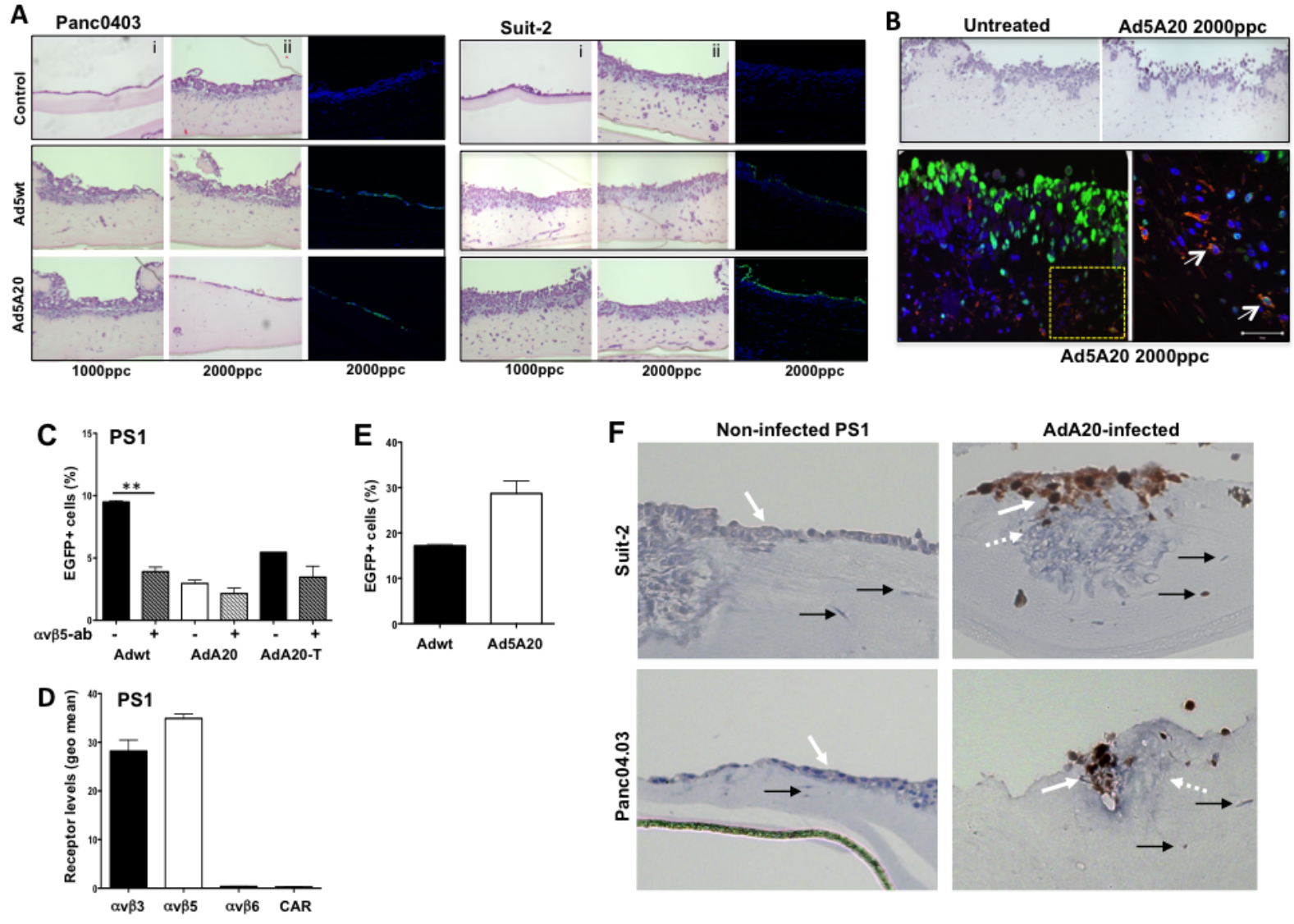
A
Panc0403
Suit-2
i
ii
Control
Ad5wt
Ad5A20
1000ppc
2000ppc
2000ppc
1000ppc
2000ppc
2000ppc
B
Untreated
Ad5A20 2000ppc
Ad5A20 2000ppc
C
PS1
EGFP+ cells (%)
**
αvβ5-ab
- + - + - +
Adwt
AdA20
AdA20-T
D
PS1
Receptor levels (geo mean)
αvβ3
αvβ5
αvβ6
CAR
E
EGFP+ cells (%)
Adwt
Ad5A20
F
Non-infected PS1
AdA20-infected
Suit-2
Panc04.03

Figure 5

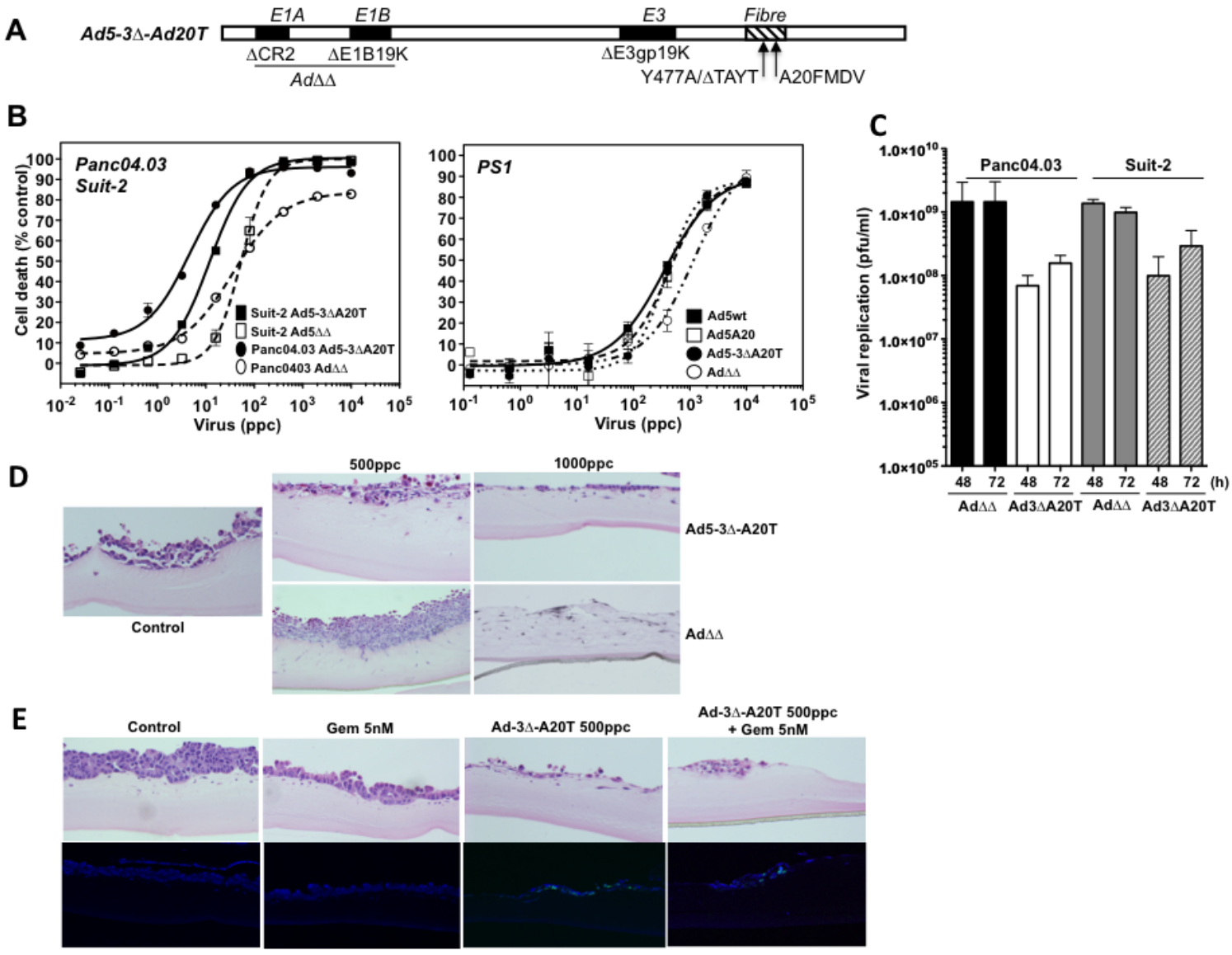
A
Ad5-3Δ-Ad20T
E1A
E1B
E3
Fibre
ΔCR2
ΔE1B19K
AdΔΔ
ΔE3gp19K
Y477A/ΔTAYT
A20FMDV
B
Panc04.03
Suit-2
Cell death (% control)
Suit-2 Ad5-3ΔA20T
Suit-2 Ad5ΔΔ
Panc04.03 Ad5-3ΔA20T
Panc0403 AdΔΔ
Virus (ppc)
PS1
Ad5wt
Ad5A20
Ad5-3ΔA20T
AdΔΔ
Virus (ppc)
C
Panc04.03
Suit-2
Viral replication (pfu/ml)
48 72 48 72 48 72 48 72 (h)
AdΔΔ
Ad3ΔA20T
AdΔΔ
Ad3ΔA20T
D
500ppc
1000ppc
Control
Ad5-3Δ-A20T
AdΔΔ
E
Control
Gem 5nM
Ad-3Δ-A20T 500ppc
Ad-3Δ-A20T 500ppc
+ Gem 5nM

Figure 6

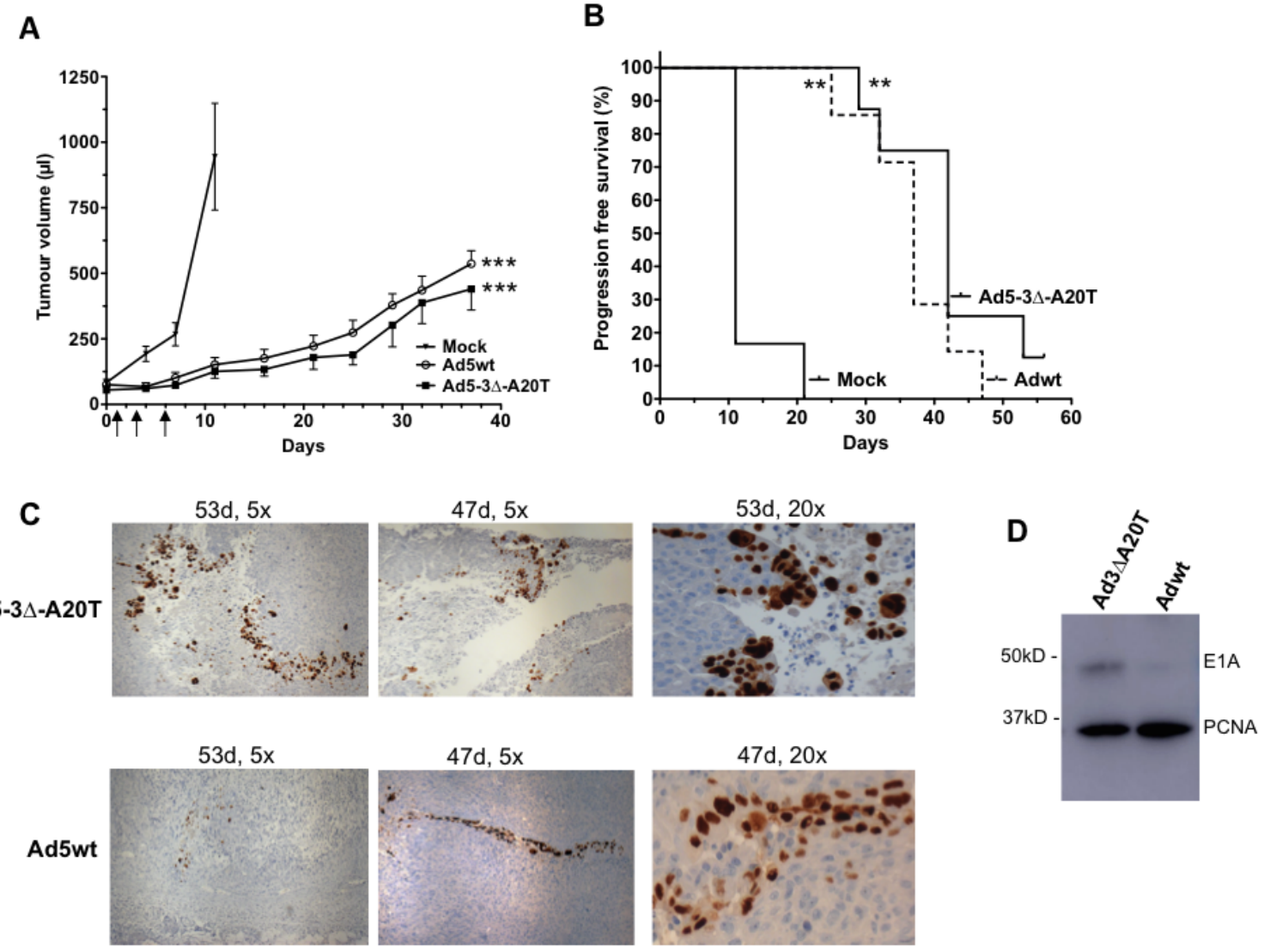
A
Tumour volume (µl)
1250
1000
750
500
250
0
0
10
20
30
40
Days
***
***
Mock
Ad5wt
Ad5-3Δ-A20T
B
Progression free survival (%)
100
90
80
70
60
50
40
30
20
10
0
0
10
20
30
40
50
60
Days
**
**
Ad5-3Δ-A20T
Mock
Adwt
C
53d, 5x
47d, 5x
53d, 20x
Ad5-3Δ-A20T
53d, 5x
47d, 5x
47d, 20x
Ad5wt
D
Ad3ΔA20T
Adwt
50kD -
37kD -
E1A
PCNA